BOHR Journal of Material Sciences and Engineering
2023, Vol. 1, No. 2, pp. 43–54
DOI: 10.54646/bjmse.2023.08
www.bohrpub.com

CASE STUDY

Tempering behavior of industrially made DP980 steel and laboratory-made DP steels and its impact on magnetic properties

J. N. Mohapatra* **and D. Satish Kumar**

JSW Steel Limited, Toranagallu, Bellary, India

***Correspondence:**
J. N. Mohapatra,
jitendra.mohapatra@jsw.in

Received: 07 September 2023; **Accepted:** 14 December 2023; **Published:** 22 December 2023

In this study hot-rolled (HR) 2.8 mm thick DP980 steel was water quenched (WQ) in laboratory from various temperatures to simulate welding-induced microstructures. The HR and WQ (925°C) samples were tempered in the temperature range 200–600°C to study the temper-induced changes in microstructure, mechanical properties, and their correlation with the magnetic properties. Microhardness, yield strength, and ultimate tensile strength of the steels were increased along with the coercivity while ductility, remanence and maximum inductions were decreased with increase in austenitization temperature for the enhancement of martensites. A reversing trend in the above properties was found with increase in tempering temperature due to the softening of the steel. However, the decreases in the properties were higher at the higher tempering temperatures in WQ samples compared to the HR samples for the stress relaxation in the steel due to reduction in density of dislocations produced during water quenching and softening of martensites.

Keywords: DP980 Steel, tempering, microstructure, mechanical properties, magnetic hysteresis loop

1 Introduction

Automotive industries are adopting ultra-high strength steels for the thickness reduction of the automotive body parts. This helps in the production of light-weight vehicles resulting in reduction in fuel consumption, reduction in CO_2 emission for environmental pollution, and enhanced safety of the occupants (1–3). For the thickness reduction of automotive components, the strength has to be higher with good ductility for the forming operations. Dual phase (DP) steels are growing in demand for their high strength and ductility. DP steel constitutes martensites embedded with ferrite matrix where martensite provides the strength while the ferrite provides the adequate ductility to the steel. With the increase in demand for strength, the martensite content is increased in different grades of DP steel to fully martensitic steel for getting the maximum strength. However, the ductility decreases with increase in strength for the increase in martensite content limiting its formability. Hence, with the process of tempering the ductility could be improved in the steels (4, 5). In addition, during welding, the microstructural changes alter the mechanical properties. Hence, monitoring such properties non-destructively will give information about the soundness of the weld. Several studies can be found on the metallurgical part of the AHSS but few studies can be found on their physical properties (6–8). More studies on physical properties and their correlation with mechanical and microstructural features will help in establishment of non-destructive evaluation methods for their non-invasive evaluation.

The microstructure, mechanical properties, and magnetic properties of hot-rolled (HR) DP980 steel and the same steel after water quenching (WQ) and temping in the range of 200–600°C were evaluated and correlated for the establishment of a non-destructive magnetic evaluation technique.

2 Materials and methods

An industrial product of hot-rolled (HR) DP980 steel strip of 2.8 mm thickness with (wt.%) 0.073C-0.171Si-3.259Mn-0.012P-0.003S was cut to 250 mm × 35 mm dimensions for further experiment. The Ar_1 and Ar_3 temperatures of the steel were calculated using the standard equations (9) and found to be 718 and 829°C, respectively. The CCT and TTT diagrams of the steel calculated using the JMatPro Software are given in **Figures1A, B**, respectively. The steels were water quenched (WQ) from soaking temperatures in the range 775–925°C with a 50°C step and a 0.5 h soaking time to soak the samples in the α + γ region and in only γ region. Three samples were used for each condition to see the scattering of properties. Additionally, six sets (6 × 3) of samples were soaked at 925°C for 0.5 h and then water quenched to generate fully martensitic structure and its tempering to study the tempering behavior along with six sets of as-received samples in a muffle furnace. Tempering was performed in the temperature range of 200–600°C with a 100°C step for 1 h soaking time followed by air cooling on both the hot-rolled and quenched conditions.

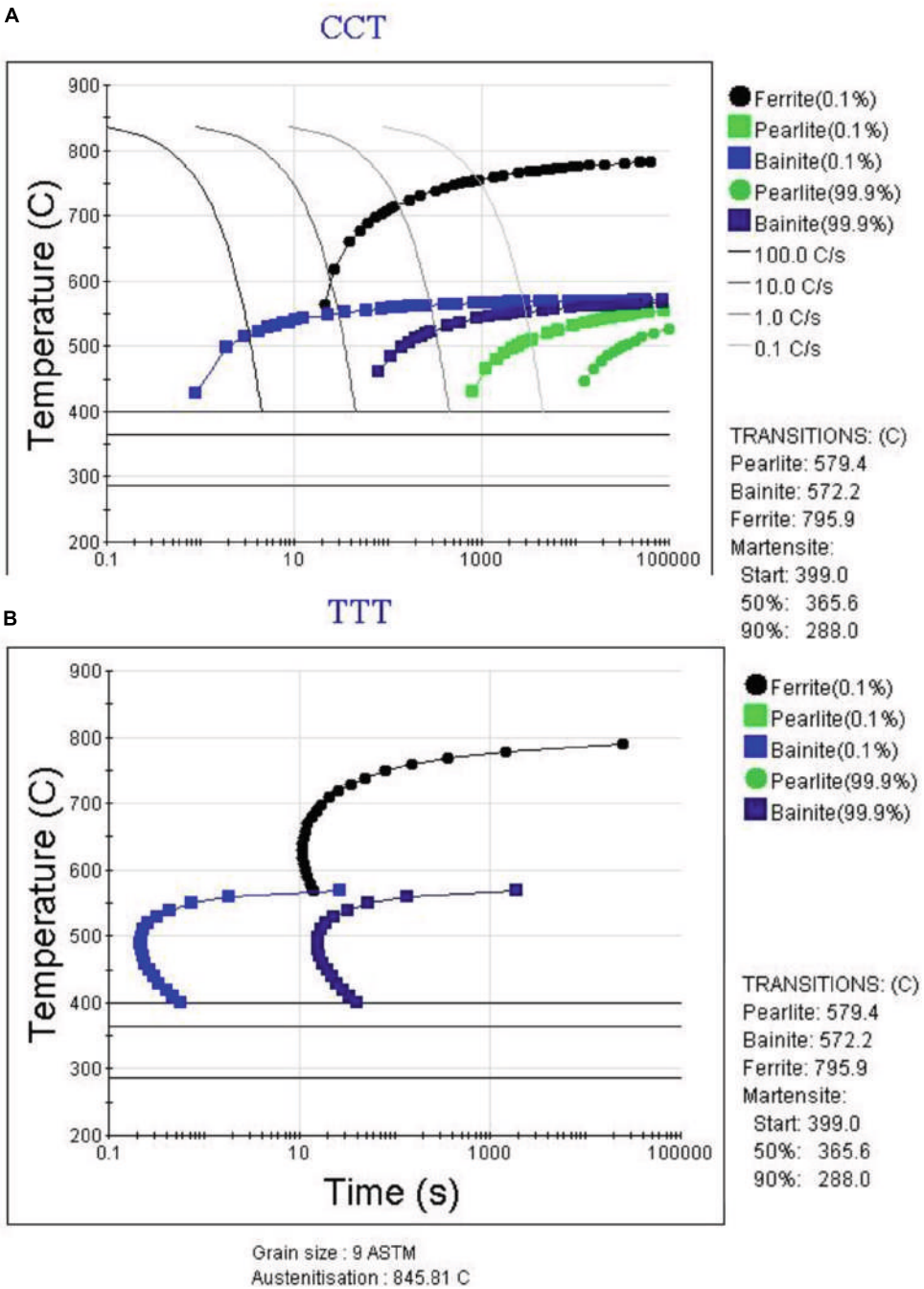

FIGURE 1 | (A) CCT and **(B)** TTT diagram of the steel.

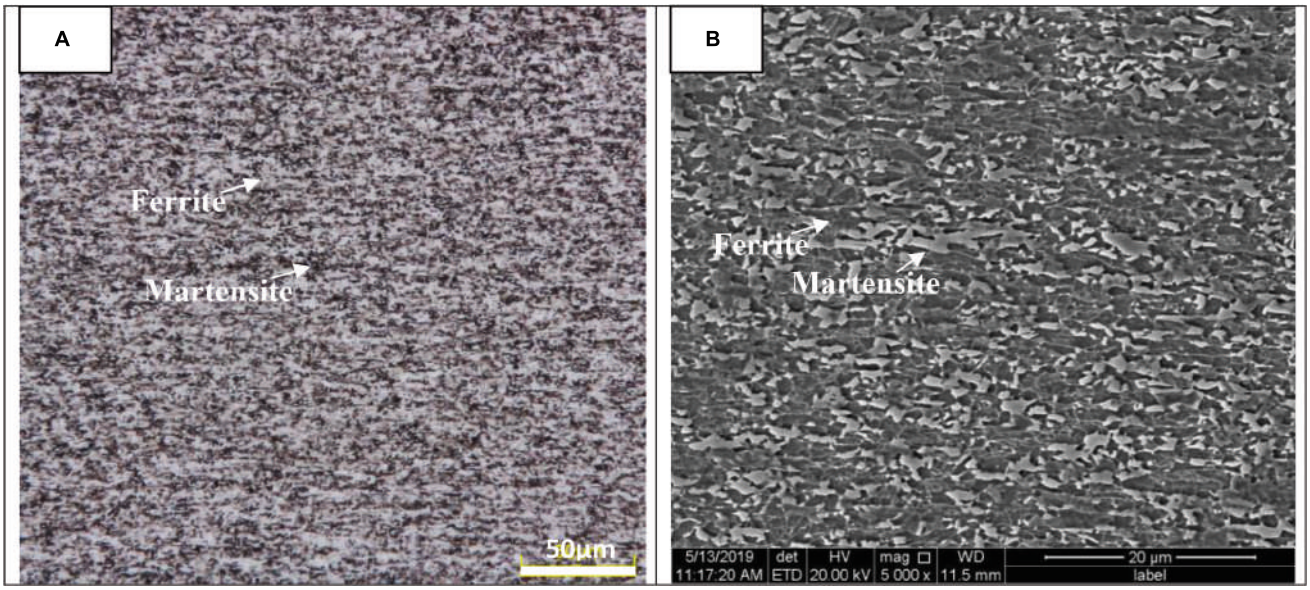

FIGURE 2 | (A) Microstructure at 1000X **(B)** SEM micrographs at 5000X of HR DP980 Steel.

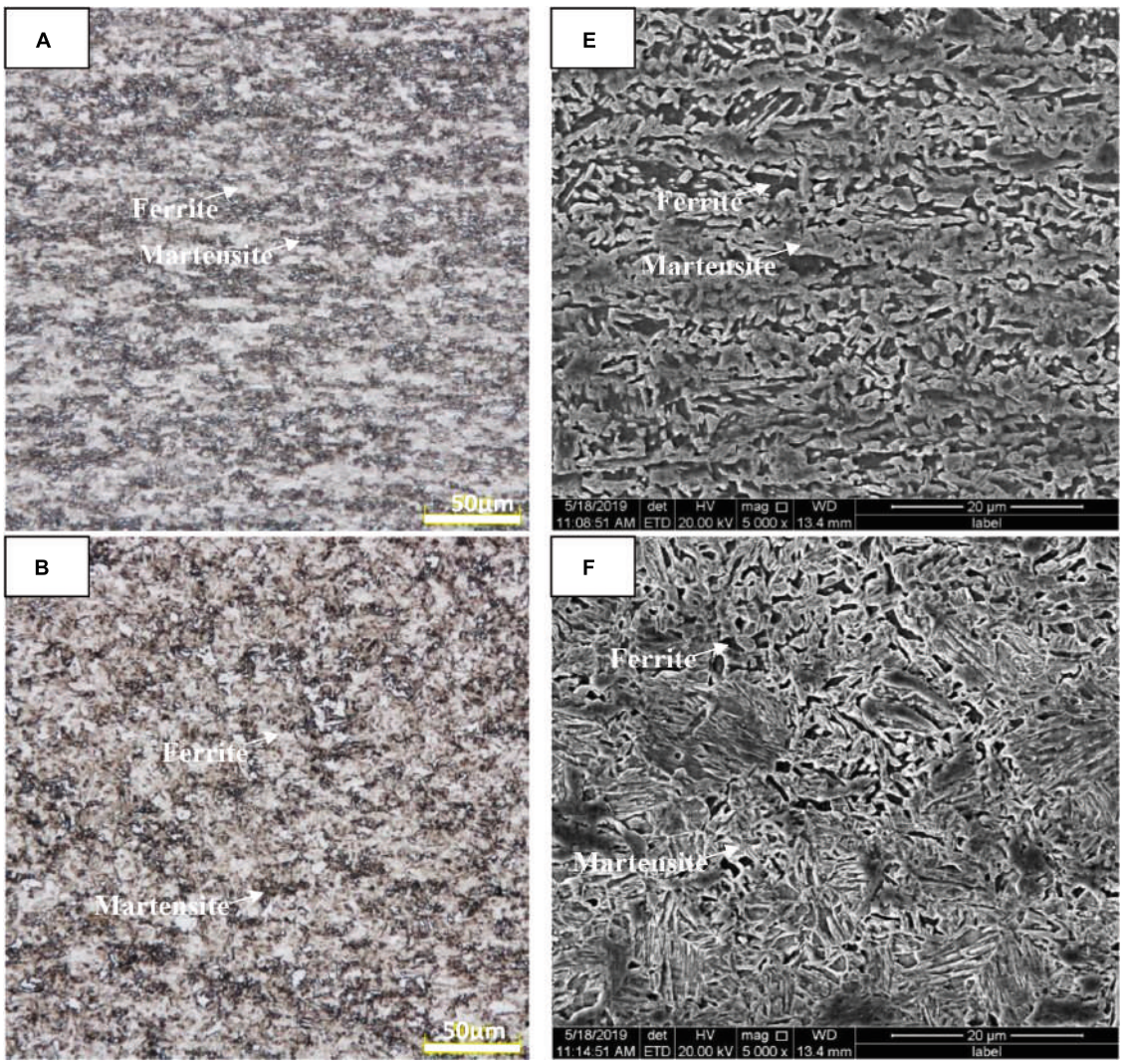

FIGURE 3 | (Continued)

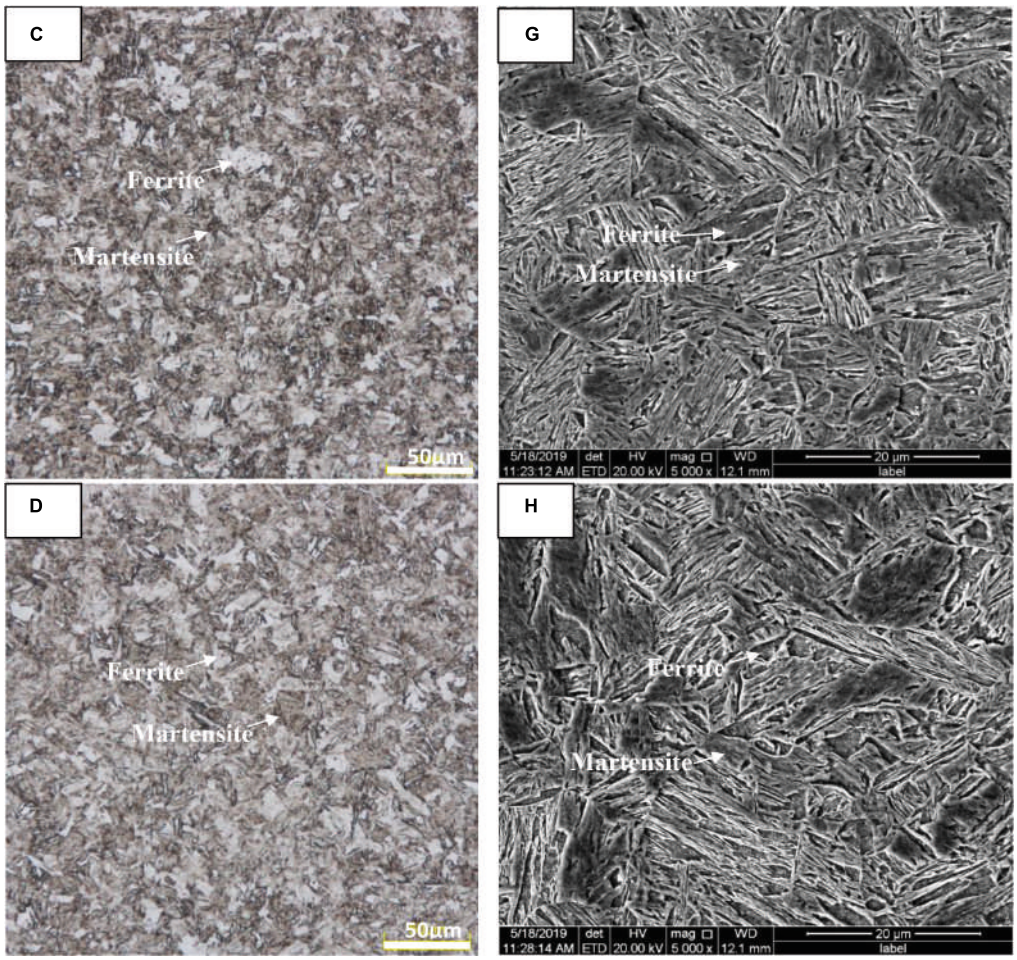

FIGURE 3 | (A–D) Microstructure at 1000X of the DP980 steel WQ from 775–925 with a 50°C step after 0.5 h soaking, **(E–H)** their corresponding SEM micrograph at 5000X.

Microstructural observations were carried out on the Nital etched specimens, using an Olympus make opto-digital microscope and a JEOL make scanning electron microscope. Micro Vicker's hardness was measured in a Vicker's hardness tester at a load of 0.5 kg. Tensile specimens were prepared according to JIS standard. Tensile tests were carried out for the measurement of mechanical properties in a Zwick/Roell make 250 kN universal tensile testing machine at a strain rate of 0.008/s. Magnetic hysteresis loop (MHL) measurements were carried out on the HR, WQ, and tempered samples, using a NDE device; *MagStar* (8). MHL measurements on HR samples and six WQ samples were done and their average and standard deviations were taken for comparison.

3 Results and discussion

3.1. Microstructure of HR and WQ DP980 Steel

Figure 2 shows the microstructure and SEM micrograph of HR DP 980 steel. The martensites are typical bulk type (dark contrast in the optical image and light contrast in SEM image) and very finer in size distributed homogeneously in the steel. The steels after WQ from various soaking

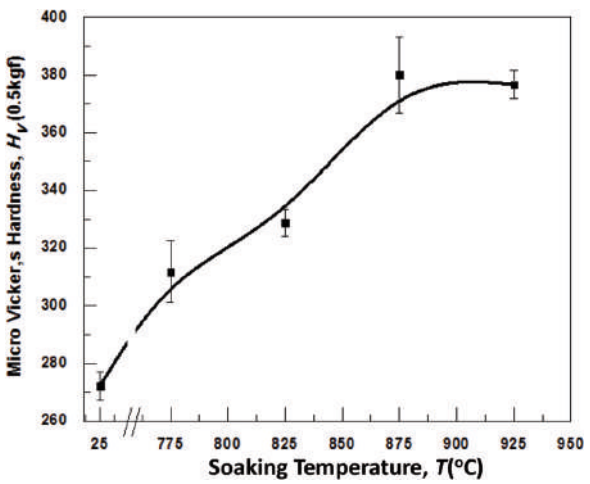

FIGURE 4 | Micro Vicker's hardness of HR and WQ steels from different soaking temperatures in the range of 775–925 with a 50°C step and 0.5 h soaking time.

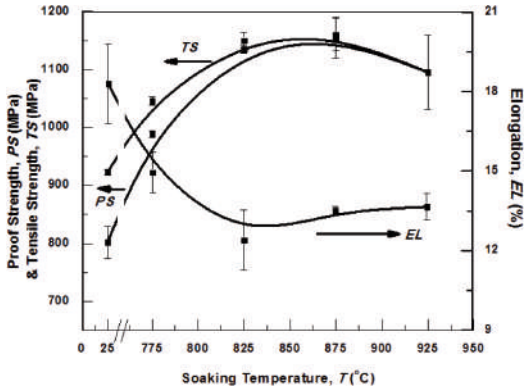

FIGURE 5 | Proof strength, tensile strength, and elongation (%) of HR and WQ steels from different soaking temperatures in the range of 775–925 with a 50°C step and 0.5 h soaking time.

temperatures are shown in **Figure 3**. The microstructure of the WQ steel after 775°C of soaking (α + γ region) also shows bulk type; however, the volume fraction of martensite phase increased with a less volume fraction of ferrite remaining. Further increase in temperature up to 825°C (α + γ region) resulted in more volume fraction of martensite. Increase in soaking temperature in the fully austenitic region (875 and 925°C) led to formation of lath type of martensites. A similar trend in martensite formation has been reported in earlier works (8, 10).

3.2. Mechanical properties of HR and WQ DP980 steel

The Micro Vicker's hardness of DP 980 steel on HR and that of WQ steel are shown in **Figure 4**. The hardness increased in the steel with increase in soaking temperature due to the increase in volume fraction of martensites due to the lattice distortion and showed a small decrease at 925°C of soaking, which might be due to the lath coarsening. The proof strength (PS), tensile strength (TS), and percentage of elongation (EL, %) of as-received and water-quenched samples are shown in **Figure 5**. The PS & TS were increased while EL was decreased with increase in soaking temperature due to the formation of fresh martensites in the steel. The transformation of ferrite to austenite at the austenization temperatures again transformed to martensite during water quenching resulted in increase in volume of the steel and produces lot of strain fields in the ferrite matrix (11). High densities of dislocations are jumbled at the ferrite–martensite grain boundary due to the transformation of austenite to martensite for the increase in volume of the steel (12, 13). At higher soaking temperatures the PS & TS are slightly decreased with small increase in EL. At higher soaking temperature the decrease in strength might be due to the formation of coarser lath type martensites.

3.3. MHL properties of HR and WQ DP980 steel

The coercivity, remanence, and maximum induction of HR and WQ steels from different soaking temperatures in the range of 775–925°C are shown in **Figure 6**. Coercivity increased while remanence and maximum induction were decreased with increase in soaking temperature. At higher soaking temperature the coercivity was decreased. During magnetization of ferromagnetic materials such as steel, the magnetic domain interacts with the pinning densities such as

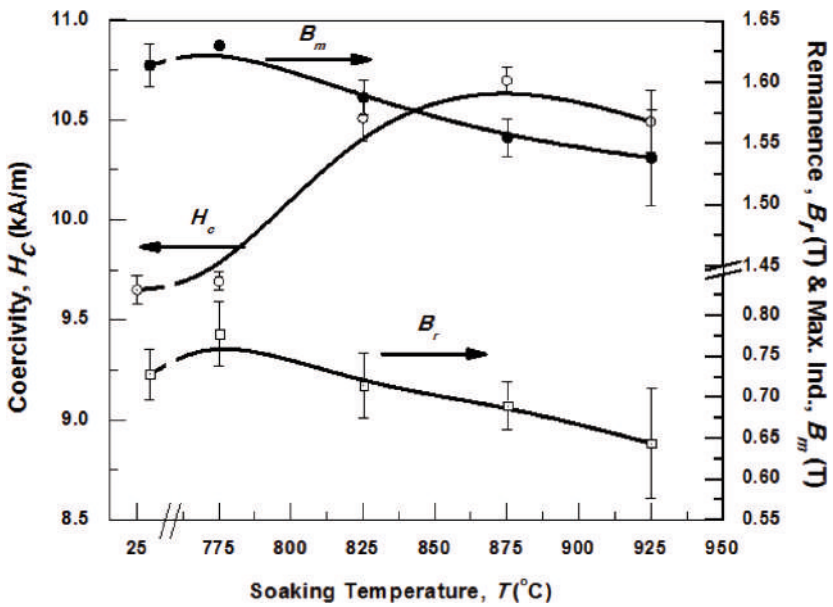

FIGURE 6 | Coercivity, remanence, and maximum induction of HR and WQ steels from different soaking temperatures in the range of 775–925 with a 50°C step and 0.5 h soaking time.

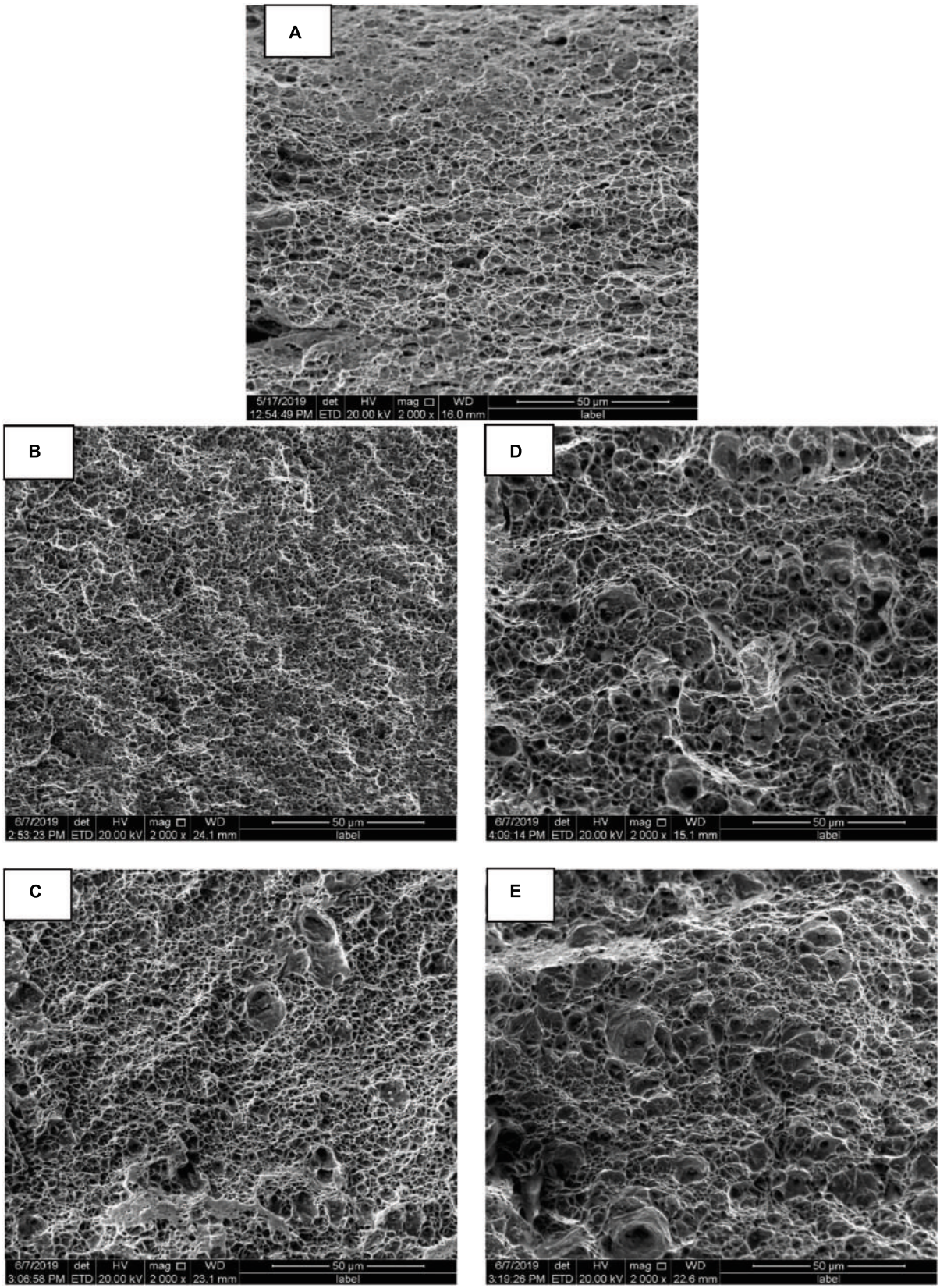

FIGURE 7 | Fracture surface of **(A)** HR and **(B)-(E)** WQ steels in the range of 775–925^{O}C with a 50°C step and 0.5h holding time.

grain boundary, precipitates, secondary phase, dislocations, and residual stress. The increase in pinning density strongly restricts the magnetic domain wall motion resulting in increase in coercivity. In this study the magnetic domain walls experienced strong pinning by the increase in volume fractions of martensites and compressive residual stress in the steel due to rapid cooling resulting in increase in coercivity. At higher soaking temperatures (925°C) due to coarsening of the lath martensite stress relaxation occurs resulting in ease for magnetic domain wall movement leading to small decrease in coercivity. The decreases in remanence and maximum inductions are due to the increase in volume fraction of martensite, which has a lower magnetic moment compared to the ferrite (14). A similar result was also reported in our earlier work on 590 MPa DP steel (8).

3.4. Fractography of HR and WQ DP980 steel

Fractography images of the HR and WQ steels are shown in **Figure 7**. The fracture surface shows dimples indicating ductile fracture of the steels. In the as-received sample fully dimple networks are seen. The dimple size is smaller for WQ samples at relately low austenitization temperature (775°C) condition and the dimple and void sizes increase with increase in soaking temperature.

3.5 Microstructure of tempered HR and WQ DP980 steel

SEM micrographs of HR and WQ (925°C/0.5 h/WQ) steel after tempering are shown in **Figure 8(A–E)** and **(F–J)**, respectively. The fine structure of martensites is homogeneously distributed in the ferrite matrix in the as-received DP980 steel and martensite structures are found to be coarsened with increase in tempering temperature. In the quenched steel the lath martensitic structures are found to be decomposed with formation of some carbides and the existing laths are coarsened. The decomposition of martensite and formation of carbides are reported earlier (15). During tempering stress relaxation, precipitation of carbides and dissolution of carbides in the ferrite are reported in another work (10). Carbon diffusion took place from the martensite at high temperature tempering resulting in

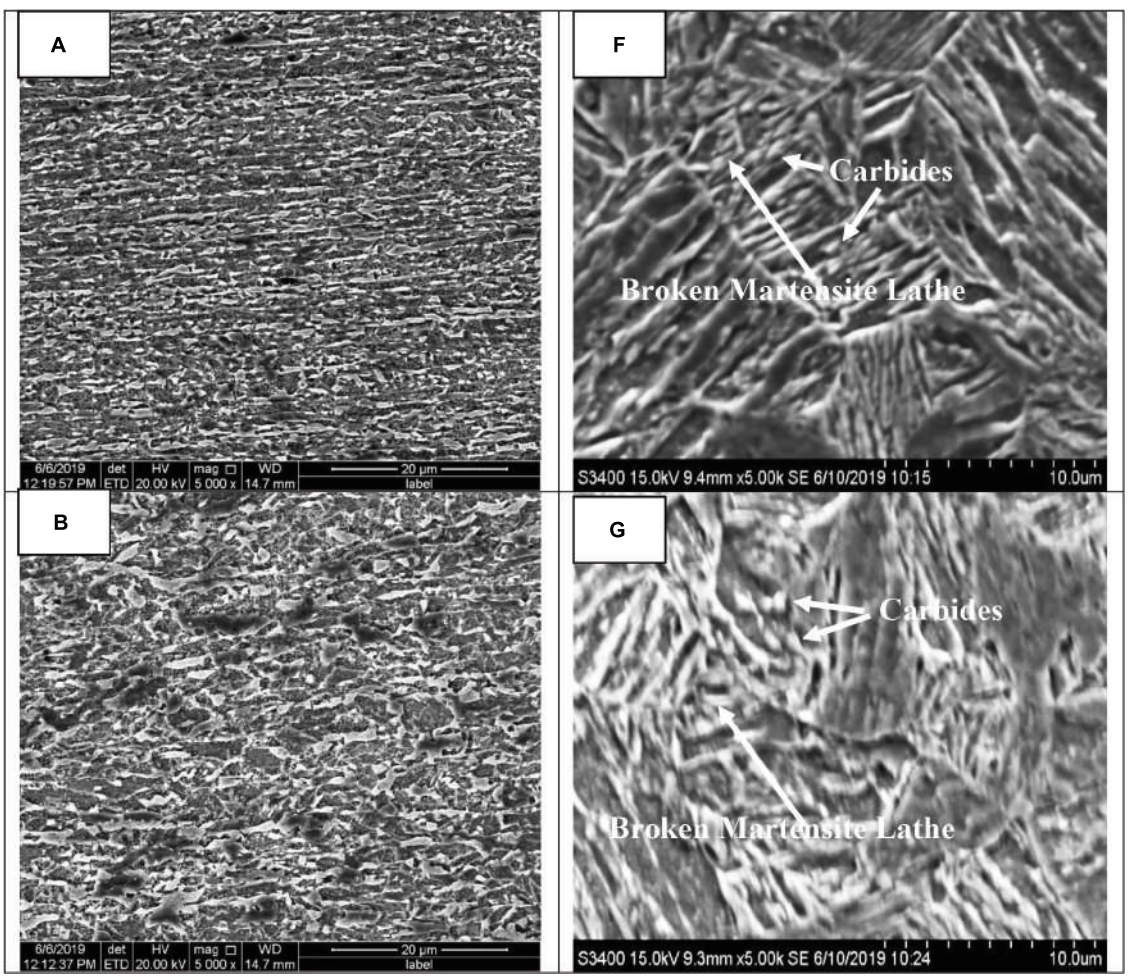

FIGURE 8 | (Continued)

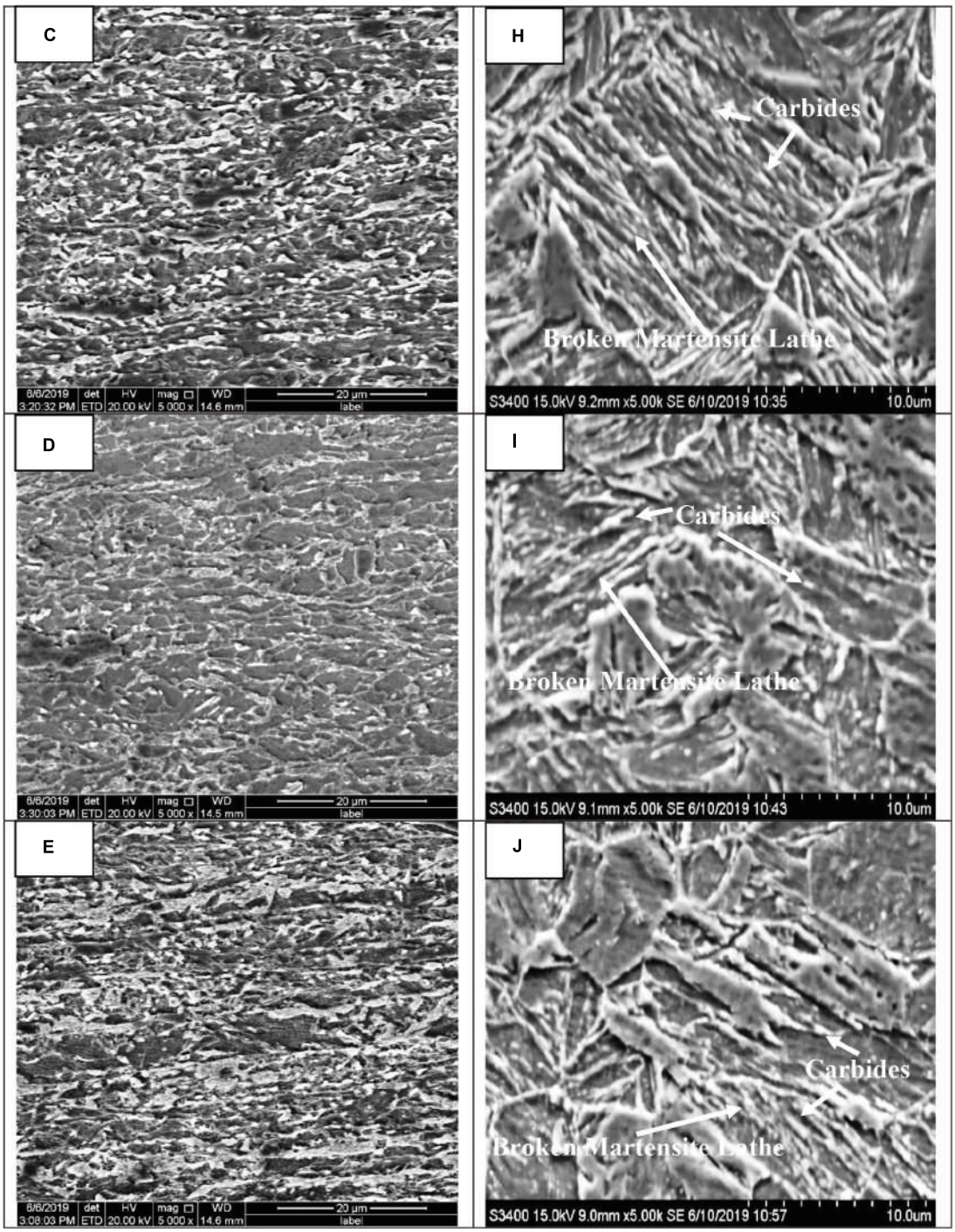

FIGURE 8 | (A–E) HR DP980 steel and **(F–J)** WQ (925°C/0.5h/WQ) steel tempered in the range of 200–600°C with a 100°C step and 1 h tempering time.

formation of fine Fe_3C carbide and ferrite (α-Fe) reported earlier (4).

3.6. Mechanical Properties of tempered HR and WQ DP980 steel

Microhardness of the HR and WQ (925°C/0.5h/WQ) steel after tempering is shown in **Figure 9**. There is a very small decrease in hardness in HR DP980 steel with tempering temperature while significant decrease is found in the WQ steel after tempering in the tempering temperature more than 300°C. Changes in PS, TS, and EL (%) of HR DP 980 steel and WQ (925°C/0.5h/WQ) DP 980 steel with tempering temperature are shown in **Figures 10 (A, B)**, respectively. Tempering resulted in decrease in PS and TS of the HR and WQ steel, while did not

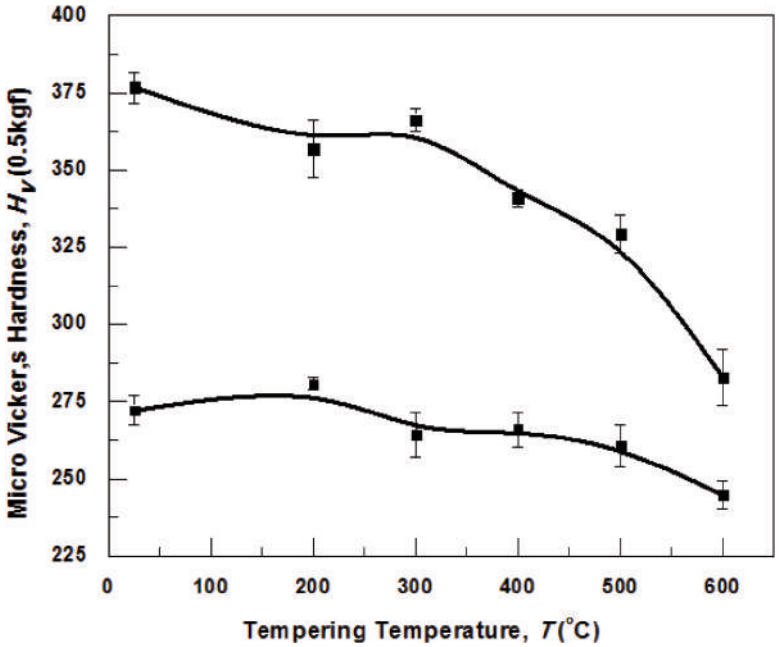

FIGURE 9 | Change in micro Vicker's hardness of the HR and WQ (925°C/0.5 h/WQ) DP 980 steel after tempering at different temperatures.

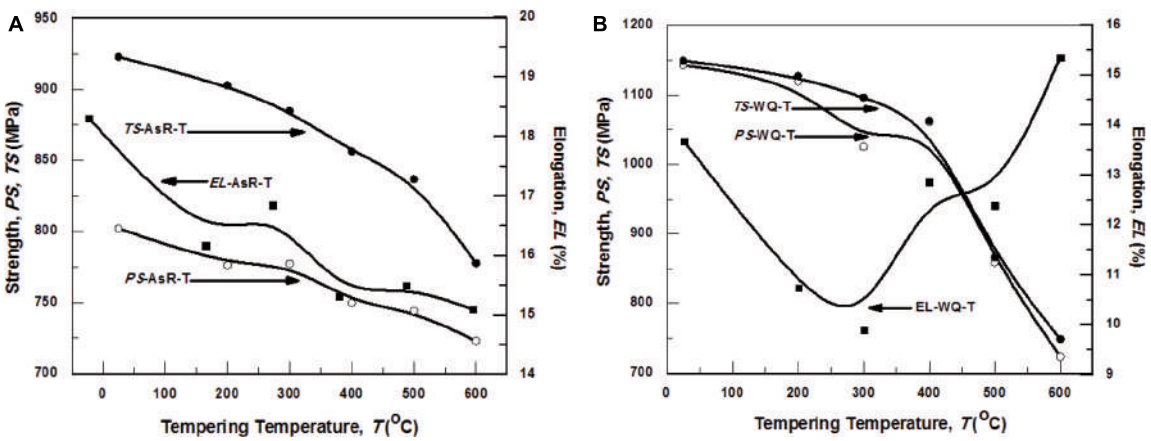

FIGURE 10 | Change in proof strength, tensile strength, and elongation (%) of **(A)** HR DP 980 steel and **(B)** WQ (925°C/0.5 h/WQ) DP 980 steel with tempering temperature.

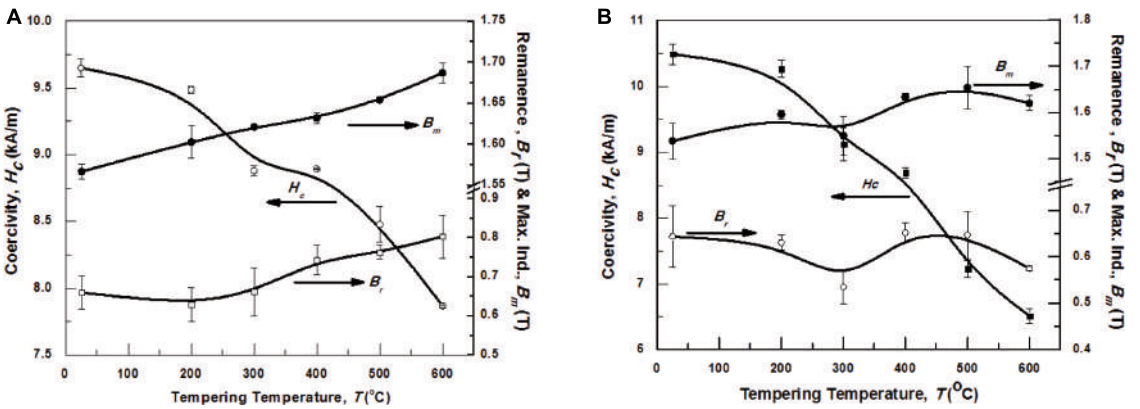

FIGURE 11 | Change in coercivity, remanence, and maximum induction of **(A)** HR DP 980 steel and **(B)** WQ (925°C/0.5 h/WQ) DP 980 steel with tempering temperature.

show significant change in elongation for HR condition and decreased with increase in tempering temperature up to 300°C and then increased with further increase in tempering temperature in the WQ steel. After 300°C of tempering, a drastic decrease in strengths and increase in elongations were found in the WQ steel, which might be due to the stress relaxation for the reduction of dislocation structure at high temperature exposure and decomposition of martensite structure in to Fe_3C carbide and α -Fe.

3.7. Magnetic properties of tempered HR and WQ DP980 steel

Changes in magnetic properties of HR and WQ (925°C/0.5 h/WQ) DP 980 steel with tempering temperature are shown in **Figures 11A, B**, respectively. Coercivity was decreased with increase in tempering temperature while the decrease was much prominent in WQ steel at higher tempering temperature compared to the HR steel similar to the change in mechanical properties in the steel. The remanence and maximum inductions were increased with increase in tempering temperature. The rapid decrease in coercivity in WQ steel is very similar to the decrease in the mechanical properties due to the relaxation of compressive residual stress and reduction of dislocation density at high-temperature exposures for the decomposition of martensite structure (16).

3.8 Fractography of tempered HR and WQ DP980 steel

Fractographic images of as-HR and WQ DP980 steel after tempering in the range of 200–600°C are shown in **Figures 12(A–E)** and **(F–J)**, respectively. The steels show dimples indicating ductile fracture of the steels. Large dimples in the fractography are indicative of

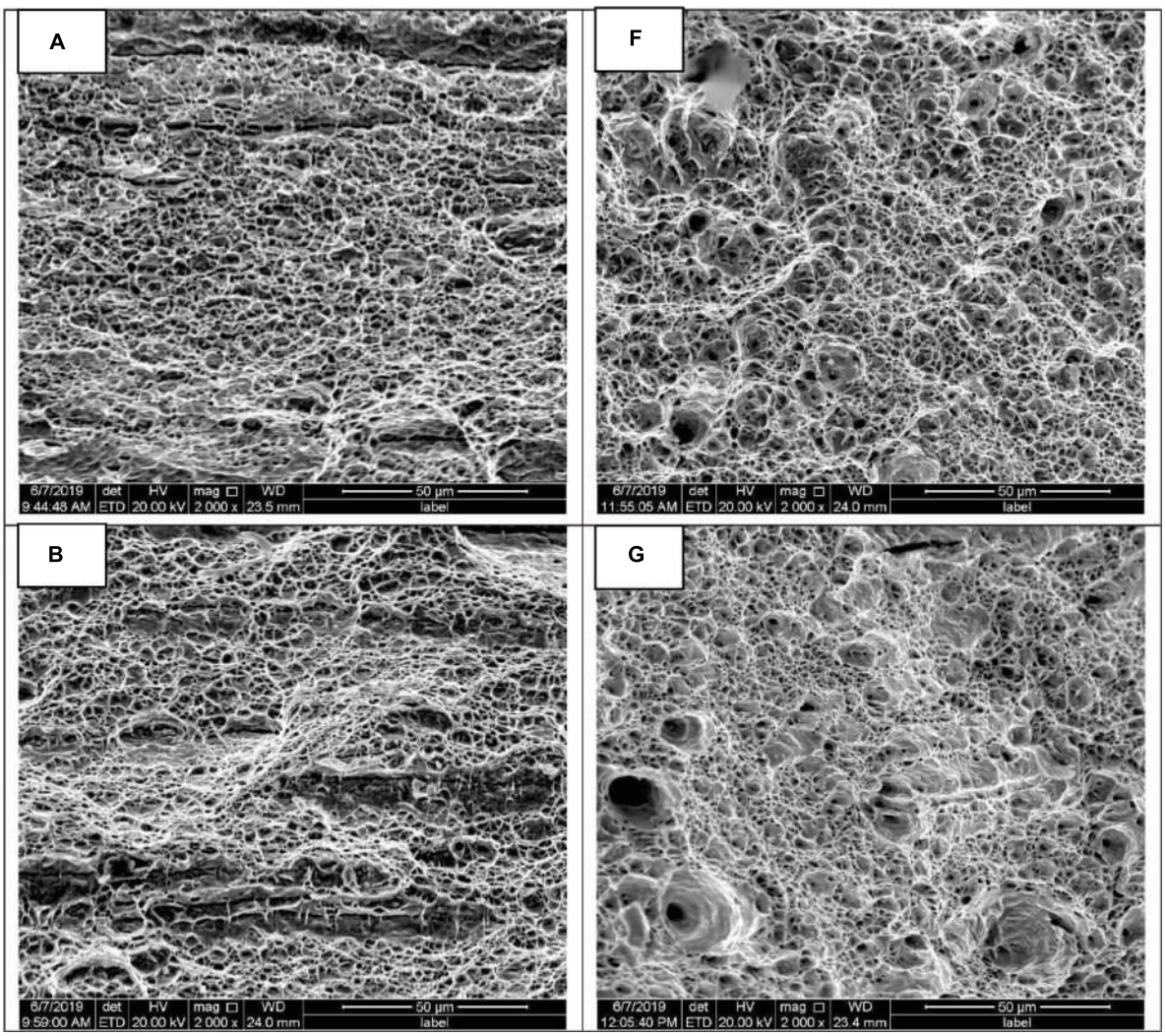

FIGURE 12 | (Continued)

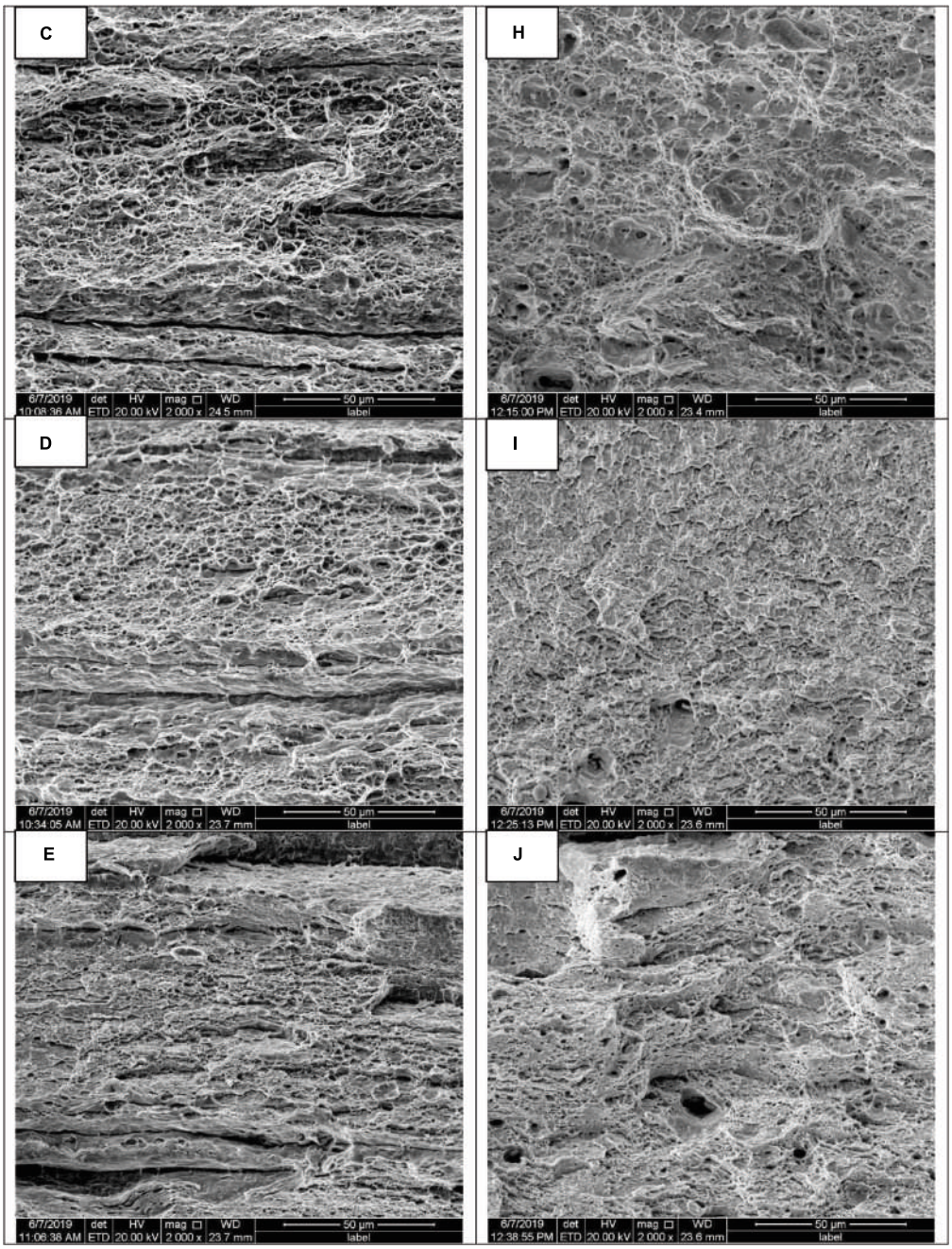

FIGURE 12 | Fractography of HR **(A–E)** and WQ **(F–J)** steel after tempering in the range of 200–600°C with a 100°C step and 1 h holding time.

improvement of ductility of the steel by tempering treatment.

4 Conclusion

Microstructure, mechanical, and magnetic hysteresis loop properties were evaluated on industrially made HR DP980 steel, WQ, and tempered DP steel with varying martensite content. It was found that the proof strength, ultimate tensile strength, and coercivity increase with increase in austenitization temperature in quenched samples for the obstructions from growing martensites. With tempering the strengths decrease along with the coercivity with increase in tempering temperature and such decreases are more at temperatures above 300°C in water-quenched sample due to the stress relaxation for the reduction in dislocation density in the material for the decomposition of martensite lath structure and lath broadening. A similar decrease in the coercivity, micro hardness and tensile strength with the microstructural modifications indicating potential non-destructive evaluation of tempering behavior of the steel through a non-destructive magnetic device.

References

1. Baluch N, Mohamed Udin Z, Abdullah CS. Advanced High Strength Steel in Auto Industry: an Overview. *Eng Technol Appl Sci Res.* (2014) 4:686–9.
2. Han Y, Kuang S, Qi X, Xie C, Liu G. Research on the Microstructures and mechaanica;l properties of Ti micro-alloyed cold rolled hot dip galvanizing DP980 steel, HSLA Steels 2015, Microalloying 2015 & Offshore Engineering Steels 2015. *Chin Soc Metals (CSM) Chin Acad Eng (CAE) TMS.* (2016).
3. Tetsuo S, Yoshimasa F, Shinjiro K. *High Strength Steel Sheets for Automobile Suspension and Chassis Use —High Strength Hot-Rolled Steel Sheets with Excellent Press Formability and Durability for Critical Safety Parts, JFE Technical Report*. (2004).
4. Sirinakorn T, Uthaisangsuk V, Srimanosaowapak S. Effects of the tempering temperature on mechanical properties of dual phase steels. *J Metals Mater Miner.* (2014) 24:13–20.
5. Li H, Gao S, Tian Y, Terada D, Shibata A, Tsuji N. Influence of tempering on mechanical properties of ferrite and martensite dual phase steel. *Mater Today Proc.* (2015) 2S:S667–71.
6. Ghanei S, Kashefi M, Mazinani M. Eddy current nondestructive evaluation of dual phase steel. *Mater Des.* (2013) 50:491–6.
7. Ghanei S, Saheb Alam A, Kashefi M, Mazinani M. Nondestructive characterization of microstructure and mechanical properties of intercritically annealed dual-phase steel by magnetic Barkhausen noise technique. *Mater Sci Eng A.* (2014) 607:253–60.
8. Mohapatra JN, Kumar S, Akela AK, Prakash Rao S, Kaza M. Magnetic hysteresis loop as a tool for the evaluation of microstructure and mechanical properties of DP Steels. *J Mater Eng Perf.* (2016) 25:2318–25.
9. Andrews KW. Empirical formulae for the calculation of some transformation temperatures. *J Iron Steel Instit.* (1965) 203:721–7.
10. Kuang CF, Li J, Zhang SG, Wang J, Liu HF, Volinsky AA. Effects of quenching and tempering on the microstructure and bake hardening behavior of ferrite and dual phase steels. *Mater. Sci Eng A.* (2014) 613:178–83.
11. Terada D, Ikeda G, Park M, Shibata A, Tsuji N. Reason for high strength and good ductility in dual phase steels composed of soft ferrite and hard martensite. *IOP Conf Ser.* (2017) 219:012008. doi: 10.1088/1757-899X/219/1/012008
12. Davis RG. Influence of martensite composition and content on the properties of dual phase steels. *Metallurg Trans A.* (1978) 9:671–9.
13. Hayat F, Uzun H. Effect of heat treatment on microstructure, mechanical properties and fracture behavior of ship and dual phase steels. *J Iron Steel Res Int.* (2011) 18:65–72.
14. Mumtaz K, Takahashi S, Echigoya J, Kamada Y. Magnetic measurements of the reverse martensite to austenite transformation in a rolled austenitic stainless steel. *J Mater Sci.* (2004) 39:1997–2010.
15. Wang S, Yu H, Zhou T, Wang L. Synergetic effects of ferrite content and tempering temperature on mechanical properties of a 960 MPa Grade HSLA Steel. *Materials.* (2018) 11:2049. doi: 10.3390/ma11102049
16. Mohapatra JN, Dabbiru SK. Magnetic evaluation of accelerated aging degradation on 2.25Cr-1Mo steel with martensitic and bainitic microstructure. *BOHR Int J Mater Sci Eng.* (2023) 1:11–9. doi: 10.54646/bijmse.2023.03